A MULTIRATE, FINITE-WIDTH, BOW-STRING INTERACTION MODEL

Stefania Serafin, Julius O. Smith III

CCRMA, Department of Music
Stanford University, Stanford, 94305 USA
`serafin@ccrma.stanford,edu`

ABSTRACT

In this paper we propose an efficient method to model the amount of bow hair in contact with the string in a physical model of a bowed string instrument.

1. INTRODUCTION

Models of bow-string interaction typically approximate the bow-string contact as a single point. However, the finite width of the bow is known to have audible effects. For example, McIntyre et al. [4] observed "differential slipping" of the bow-string contact during the sticking phase of bowed-string motion. In differential slipping, the string occasionally slips on one side of the bow while remaining stuck on the other side (or it could slide briefly in opposite directions). The authors modeled the differential slipping events using a "two-hair" bow, i.e., a bow having only two points of contact, corresponding to the bow edges. They noted that ideal Helmholtz motion requires that the string slope change from positive to negative during sticking, while the static friction of the bow-string contact attempts to prevent any slope changes under the bow; this conflict creates differential slipping, even in the case of only two bowing points. Differential slipping events generate irregular spikes in the force excerted by the string on the bridge, which in turn produce audible noise.

More recently, Pitteroff and Woodhouse [6, 7] have developed a more accurate physical model of finite-width bow-string contact using finite-difference approximations. They showed that in a complex system such as a bowed string, a point and a finite-width excitation do not produce the same kind of behaviour. Since their technique is rather expensive for real-time implementation, there remains a need for alternative solutions.

In this paper we propose an relatively efficient computational model of the finite-width bow intended for sound synthesis applications. The model produces differential slipping noise as is found in real bowed-string instruments.

2. "CLASSIC" BOW-STRING MODELS

The single-point bow-string model is classic, and a review may be found in [5]. This model approximates bow-string contact at a point which is at a normalized distance β from the bridge, where $\beta = 0.5$ represents the middle of the string. The bow velocity and the bow force at the contact point are denoted v_b and f_b, respectively. At the contact point, two physical variables are considered: the friction force f and the transverse velocity of the string v. Friction and velocity are nonlinearly related via the bow-string contact parameters [9].

When the velocity v_b of the bow is equal to that of the string v, they are "stuck together", otherwise they are sliding. The alternating sticking and sliding phases give rise to the characteristic movement of the string (known as the Helmholtz motion).

The velocity v at the contact point results from the contribution of the waves v_{i_n} and v_{i_b} coming from the nut and the bridge respectively. In the same way, two travelling waves v_{o_n} and v_{o_b} resulting from the bow string interaction propagate toward the nut and the bridge. Then we can write:

$$\begin{aligned} v &= v_{o_n} + v_{i_n} \\ &= v_{o_b} + v_{i_b} \end{aligned}$$

The contribution of the reflected waves v_{i_n} and v_{i_b} are summed at the contact point:

$$v_h = v_{i_n} + v_{i_b}$$

Bow string interaction is represented by system (1):

$$\begin{cases} f &= 2\,Z\,(v - v_h) & (1a) \\ f &= \mu\,(v - v_b) & (1b) \end{cases} \qquad (1)$$

Once this coupling has been solved, the new outgoing waves v_{o_n} and v_{o_b} are calculated by equations $(2a)$ and $(2b)$:

$$\begin{cases} v_{o_n} &= v_{i_b} + \frac{f}{2Z} & (2a) \\ v_{o_b} &= v_{i_n} + \frac{f}{2Z} & (2b) \end{cases} \qquad (2)$$

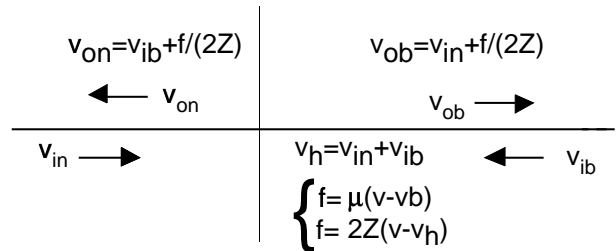The model is described in Fig. 1, and Fig. 2 presents its block structure.

Figure 1: *Description of the basic bow-string interaction model.*

In Fig. 2, f represents the frictional force, while, $H_{\text{lt}}(z)$ and $H_{\text{rt}}(z)$ are the filters that model the losses of the left-going and
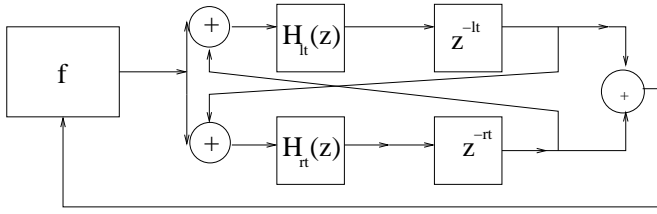
Figure 2: *Block structure of the basic bowed string model.*

right-going waves propagating toward the bridge and the nut respectively.

z^{-lt} and z^{-rt} represent the left-going and right-going delay lines respectively.

This model allows to reproduce the idealised Helmholtz motion, which is the solution of a hypothetical system of a perfect flexible string bowed in a single point by a rigid bow [1].

The following section describes how to improve this model to obtain more realistic waveforms.

3. TOWARD MORE ACCURATE BOWED STRING MODELS

3.1. Accounting for torsional waves

To refine the bowed string model introduced in the previous section, we need to take into account other physical effects.

The first one consists of accounting for the torsional waves. Since torsional damping is greater rate than transversal damping, including torsional waves in the model allows the Helmholtz motion to establish quicker ([2]). For a description of how torsional waves can be included in the model, see, e.g., [5].

3.2. Modeling the stiffness of the string

A second improvement consists of accounting for stiffness, whose main role is to disperse the sharp corners that characterize the ideal Helmholtz motion.

As described in [8], stiffness can be modeled using allpass filters whose coefficients are obtained minimizing the infinity norm of the error between the internal loop of the string and the approximation by the filter's cascade.

The structure of the more accurate model of a bowed string is represented in Fig. 3.

In Fig. 3, as before, f represents the frictional force, while, $H_{lt}(z)$ and $H_{rt}(z)$ are the filters that model the losses of the left-going and right-going transversal waves propagating toward the bridge and the nut respectively.

z^{-lt} and z^{-rt} represent the left-going and right-going delay lines respectively. In addition to the structure of Fig. 2, $H_{ltr}(z)$ and $H_{rtr}(z)$ are the filters that model the losses of the left-going and right-going torsional waves propagating toward the bridge and the nut respectively.

Moreover, z^{-ltr} and z^{-rtr} represent the left-going and right-going delay lines for the transversal waves, and $H_a(z)$ represent the cascade of allpass filters used to model dispersion.

The model just described is able to simulate the rounding off of the idealised waveform by introducing more dissipative terms and dispersive terms.
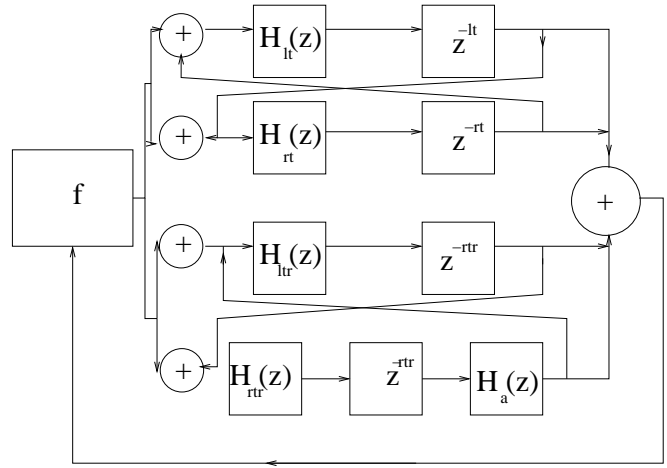

Figure 3: Structure of a refined model of a bowed string, which accounts for torsional waves and stiffness of strings.

In the next section we describe how the model can be further refined to account for the finite bow width, which is incompatible with the ideal Helmholt motion.

4. A TWO POINT BOW-STRING INTERACTION MODEL

Since the transitions from stick to slip are not instantaneous, different regions across the bow may have different release and capture events, and a situation called "differential-slipping events" described in [4] can occur. In differential slipping, bow hairs near the bridge may slip backward relative to the bow motion, while bow hairs on the nut side may slip forward. This process can be understood as the string "straightening out" under the bow as the bowing point moves uniformly from one extreme (capture) to the other (release).

Helmholtz motion is generally not disrupted by differential slipping due in part to the damping provided by torsional string motion and the finite compliance of the bow-hair.

Differential slipping can create audible events, especially when bowing closer to the bridge.

To account for differential slips we propose a two point model that allows us to simulate efficiently the finite width of the bow. As shown in Fig. 4, the bow is in contact with the string in two points called v_{hl} and v_{hr}. The contact point v_{hl} on the left side of the bow is obtained summing the contribution coming from the left side of the bow, plus a filtered version of the wave coming from the right side, which is attenuated by the bow air. The same is true for the contact point on the right side, denoted by v_{hr}, so we can write:

$$\{ \quad v_{hl} = v_{i_n} * h_r + v_{i_b} \qquad v_{hr} = v_{i_n} + v_{i_b} * h_l \qquad (2)$$

where h_r and h_l are two filters that model the right and left side attenuation respectively.

So two bow-string interactions have to be solved, one for each side of the bow, which give two friction values as:

$$\begin{cases} f_l = 2 Z (v_l - v_{hl}) & (3a) \\ f_l = \mu (v_l - v_b) & (3b) \end{cases} \qquad (3)$$

and

$$\left\{ \begin{array}{rcll} f_r & = & 2\,Z\,(v_r - v_{hr}) & (4a) \\ f_r & = & \mu\,(v_r - v_b) & (4b) \end{array} \right. \qquad (4)$$

where f_l and f_r represent the values of the friction calculated at the left and the right side of the bow respectively, and v_l and v_r represent the velocity at the left and right contact point respectively.

This allows to calculate the new outgoing velocites as follows:

$$\left\{ \begin{array}{rcll} v_{o_n} & = & v_{i_b} + \frac{f_r}{2Z} & (4a) \\ v_{o_b} & = & v_{i_n} + \frac{f_l}{2Z} & (4b) \end{array} \right. \qquad (5)$$
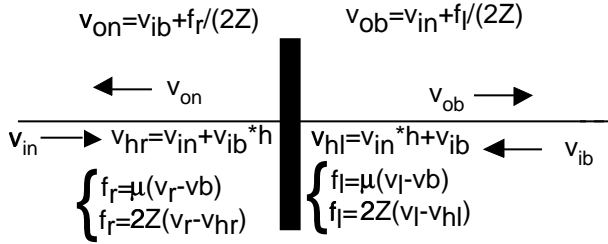
Figure 4: *Structure of the two point bow-string interaction model*

5. THE BOW HAIR

The ribbon of bow-hair on a violin bow consists of approximately 200 hairs, of which normally 50 or so are in immediate contact with the string [7].

Since the distance between the hairs is smaller than the wavelength, we can approximate the bow hair as a uniform material.

6. CONVERSION OF PHYSICAL PARAMETERS TO SAMPLES

Since the diameter of an individual bow hair is about 0.2 mm, and no more than 50 hairs are in contact with the string, the resulting bow width is about 1 cm. This means that at an audio rate of 44100 Hz the number of samples corresponding to the bow width is given by $(44100/f_0) * \delta/l$, where δ represents the width of the bow, l is the length of the string (0.69 m) and f_0 is the fundamental frequency of the string. For example, in the case of a violin G string, we have $f_0 = 196$ Hz, which gives a bow of three samples in contact with the string.

On the other end, a violin E string ($f_0 = 659$ Hz) gives less than one sample of contact area.

To cope with this problem, we use a multirate model, as described in the following section.

7. A MULTIRATE BOW HAIR MODEL

We use digital fractional delays ([10, 3]) which allow both a fine tuning of the sampling instants and an efficient implementation of sample rate conversion.

The output samples are computed with different delay values, according to the corresponding string that is played.
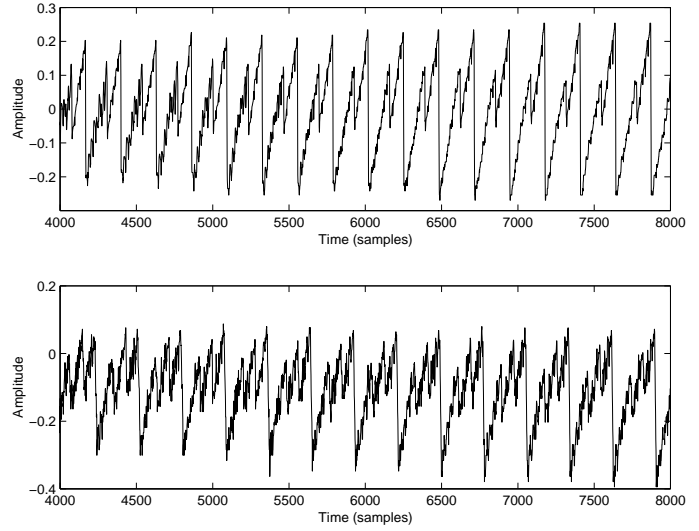
Figure 5: *Motion of a bowed string with the bow excited at normalized bow position of 0.07. Top: basic model, bottom: model that accounts for the bow width.*

For example, we associate the standard audio rate of 44.1 kHz with the G string, which, as explained before, gives 3.26 samples of full contact.

Having the same number of samples for the highest violin string (i.e., the E string, at 659 Hz), would require a sample rate of about 140kHz, which is way above the usual standards.

On the other hand, imposing a sample rate of about 48 kHz would result in a single sample of bow hair contact, which reduces the two point model to the single point model.

Our compromise consists of choosing a sample rate of 82 kHz for the E string, which gives about 1.8 samples of full contact, and allows to excite also the higher harmonics of the string to obtain brighter sonorities without encountering aliasing.

8. SIMULATION RESULTS

Figure 6 shows the waveforms captured by the different models after reaching steady state, about 4000 samples from the attack, when the Helmholtz motion is established.

These simulations show a cello G string bowed with a constant bow force of 0.2 N and a constant bow velocity of 0.05 m/s. The bow was placed at a normalized distance from the bridge of 0.1, where 0 represents the bridge while 1 represents the nut.

The top figure represent the waveforms created by the basic model of Fig. 2. The second figure from the top represents the basic model with torsional waves. The third figure is the model with torsional waves and allpass filters to account for inharmonicity. Finally, the bottom figure represents the model with the same features as the previous one, but with the bow width model included.

Notice how the Helmholtz waveform is somehow more "noisy" than in the previous examples. These perturbations result in audible noise, qualitatively similar to that in real bowed string instruments. Figure 5 shows how the noise-generated spikes in the waveform are even more evident when bowing closer to the bridge. Maintaining the same parameters as in Fig. 6, we move the bridge to a normalized distance of 0.07.
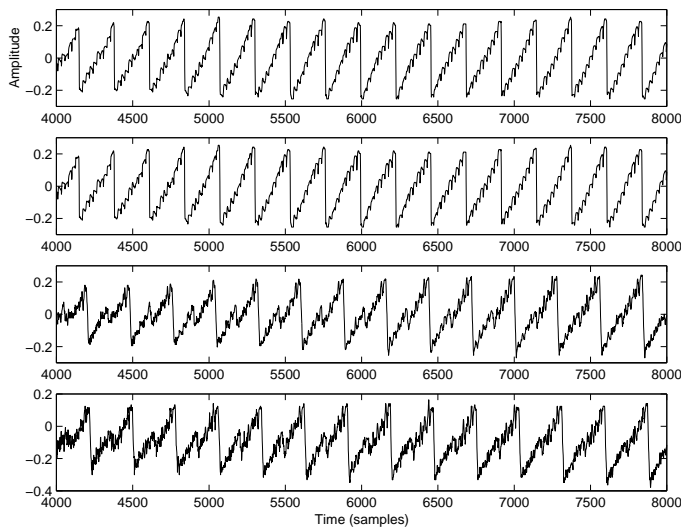
Figure 6: *Motion of a bowed string obtained using different models. From top to bottom: basic model, basic model with torsional waves, basic model with torsional waves and string stiffness, model with torsional waves, string stiffness and bow width.*

9. TILTING THE BOW

Having a bow of finite width allows to reproduce the movement of the player while tilting his bow simply by changing the number of "bow samples" in contact with the string.

Moreover, it is possible to simulate bows whose width is larger than that of a real instrument, simply by increasing the amount of samples that represent the contact area.

10. RESULTS AND FUTURE WORK

In this paper, we have proposed a method for bow width simulation which provides the characteristic noise of bowed string instruments due to differential slipping. For the future, we are studying ways to improve our two-point model toward more accurate models, such as the Pitteroff-Woodhouse model, so as to provide higher realism while keeping the computational expense reasonable.

11. REFERENCES

[1] L. Cremer. *The Physics of the Violin*. MIT Press, Cambridge, MA, 1984.

[2] S.J. Elliot F.S. Gillan. Measurements of the torsional modes of vibration of strings on instruments of the violin family. *Journal of Sound and Vibration*, 130:347–351, 1989.

[3] Timo I. Laakso, Vesa Välimäki, Matti Karjalainen, and Unto K. Laine. Splitting the Unit Delay—Tools for Fractional Delay Filter Design. *IEEE Signal Processing Magazine*, 13(1):30–60, January 1996.

[4] Michael E. McIntyre, Robert T. Schumacher, and James Woodhouse. Aperiodicity in bowed-string motion. *Acustica*, 49(1):13–32, Sept. 1981.

[5] Michael E. McIntyre, Robert T. Schumacher, and James Woodhouse. On the oscillations of musical instruments. *Acoustical of America*, 74(5):1325–1345, Nov. 1983.

[6] R. Pitteroff. Modelling of the bowed string taking into account the width of the bow. In *Stockholm Musical Acoustics Conference (SMAC-93)*, pages 407–410, Stockholm, July 1993. Royal Swedish Academy of Music.

[7] R. Pitteroff. Mechanics of the contact area between a violin bow and a string. part i:reflection and transmission behaviour. part ii: Simulating the bowed string. part iii: Parameter dependance. In *Acustica-Acta Acustica*, pages 543–562, 1998.

[8] Stefania Serafin and Julius O. Smith, III. Modelling stiffness in virtual bowed string instruments. In *Proceedings*, Atlanta meeting, june 2000. Acoustical Society of America.

[9] Jonathan H. Smith and James Woodhouse. The tribology of rosin. Part I: Dynamic friction measurements. Part II: Thermal modelling. Part III: Stick-slip simulation. in preparation.

[10] Vesa Välimäki, Matti Karjalainen, and Timo I. Laakso. Fractional delay digital filters. In *Circuits and Systems (ISCAS-93), Chicago*, New York, May 1993. IEEE Press.